Journal of Microbiological Methods 107 (2014) 161–168

Contents lists available at ScienceDirect

Journal of Microbiological Methods

journal homepage: www.elsevier.com/locate/jmicmeth

A method for sampling microbial aerosols using high altitude balloons

N.C. Bryan [a], M. Stewart [b], D. Granger [b], T.G. Guzik [b], B.C. Christner [a,*]

[a] Department of Biological Sciences, Louisiana State University, Baton Rouge, LA 70803, USA
[b] Department of Physics and Astronomy, Louisiana State University, Baton Rouge, LA 70803, USA

ARTICLE INFO

Article history:
Received 7 August 2014
Received in revised form 6 October 2014
Accepted 11 October 2014
Available online 22 October 2014

Keywords:
Balloon sonde sampling
Bioaerosols
Troposphere
Stratosphere
Microbial decontamination

ABSTRACT

Owing to the challenges posed to microbial aerosol sampling at high altitudes, very little is known about the abundance, diversity, and extent of microbial taxa in the Earth-atmosphere system. To directly address this knowledge gap, we designed, constructed, and tested a system that passively samples aerosols during ascent through the atmosphere while tethered to a helium-filled latex sounding balloon. The sampling payload is ~2.7 kg and comprised of an electronics box and three sampling chambers (one serving as a procedural control). Each chamber is sealed with retractable doors that can be commanded to open and close at designated altitudes. The payload is deployed together with radio beacons that transmit GPS coordinates (latitude, longitude and altitude) in real time for tracking and recovery. A cut mechanism separates the payload string from the balloon at any desired altitude, returning all equipment safely to the ground on a parachute. When the chambers are opened, aerosol sampling is performed using the Rotorod® collection method (40 rods per chamber), with each rod passing through 0.035 m^3 per km of altitude sampled. Based on quality control measurements, the collection of ~100 cells rod^{-1} provided a 3-sigma confidence level of detection. The payload system described can be mated with any type of balloon platform and provides a tool for characterizing the vertical distribution of microorganisms in the troposphere and stratosphere.

1. Introduction

Microorganisms aerosolized from the Earth's surface are transported both vertically (Fulton, 1966) and horizontally (Burrows et al., 2009; Griffin et al., 2001) in the atmosphere. Cells with an aerodynamic diameter less than 10 μm are geographically disseminated over long distances and have been shown to retain their viability after intercontinental transport (Griffin et al., 2006; Hara and Zhang, 2012; Murata and Zhang, 2014; Smith et al., 2012; Smith et al., 2013). Certain microbes may even retain their metabolic function in the atmosphere (Sattler et al., 2001; Vaïtilingom et al., 2011) or have active roles in meteorological processes such as ice nucleation (Christner et al., 2008; Joly et al., 2014) or cloud formation (Bauer et al., 2002; Pöschl et al., 2010).

Sampling microorganisms in the troposphere and stratosphere is challenging, and consequently, there are very few data available on the concentration and nature of microbial life in the high atmosphere. There are reports of viable microorganisms isolated from samples collected from 20–77 km above sea level (hereafter, all altitudes referenced above sea level; Griffin, 2004; Griffin, 2008; Harris et al., 2002; Imshenetsky et al., 1978; Shivaji et al., 2006; Smith et al., 2010; Yang et al., 2008); however, there are quantitative data only for altitudes below 10 km (Amato et al., 2005; DeLeon-Rodriguez et al., 2013; Huffman et al., 2010; Huffman et al., 2012; Vaïtilingom et al., 2012). Conclusions based on observations of microbial growth from samples collected at altitudes at or above 41 km (e.g., Wainwright et al., 2003; Imshenetsky et al., 1978) have resulted in extraordinary claims for the tenacity of life in the stratosphere and mesosphere. However, the aforementioned studies have lacked rigorous measures to exclude the possibility of microbial contamination, and to date, these observations have not been verified.

Here we report on an autonomous balloon sonde system for sampling bioaerosols to altitudes in the stratosphere. Environmental conditions at high altitude make standard aeromicrobiological sampling approaches challenging, necessitating the use of technology that functions under low extremes of pressure and temperature. Since the concentration of bioaerosols is anticipated to decrease with altitude, high sensitivities are required to exceed the signal to noise ratio threshold. Therefore, reduction and assessment of microbial contamination associated with system components and sampling substrates are a very relevant aspect of these measurements. We discuss the application of our bioaerosol sampling approach for studies interested in examining the geographic boundaries of microbial dispersal via the atmosphere, defining the upper altitude limits for life in the biosphere, and assessing habitability in extraterrestrial atmospheres.

2. Materials and methods

2.1. Balloon vehicle

The vehicle used to carry the Life's Atmospheric Microbial Boundary (LAMB) bioaerosol sampling payload to stratospheric altitudes up to

* Corresponding author.
E-mail address: xner@lsu.edu (B.C. Christner).

http://dx.doi.org/10.1016/j.mimet.2014.10.007
0167-7012/

38 km consisted of a 2.0-kg latex sounding balloon, a parachute, a flight termination unit, the primary radio beacon, and a video camera. The total weight suspended below the balloon is about 5.4 kg and all balloons were inflated with helium to achieve an initial ascent rate of about 350 m per minute. The balloon carried all components up to a pre-programmed cut altitude, at which point the flight termination unit triggers. When triggered, the termination unit melts a nylon string connecting the balloon to the top of the parachute, releasing the balloon and allowing the payload components to descend by parachute for recovery.

The primary radio beacon includes a Trimble Copernicus II global positioning system (GPS) receiver and Byonics Micro-Trak RTG FA High Altitude Combo transmitter to report the real-time latitude, longitude, and altitude of the balloon vehicle throughout the flight. The beacon broadcasts these data using an Automatic Packet Reporting System (APRS) communication on frequency 144.390 MHz. This system allows the balloon vehicle to be continuously tracked over a very wide area from a fixed ground location or mobile station. During payload flight operations, two ground vehicles were outfitted with a radio transceiver and laptop tracking system capable of receiving the APRS packets and mapping the beacon location. This enabled the ground crew to follow the balloon vehicle and quickly reach the landing site for payload recovery.

Located above the LAMB payload is a Kodak Zx1 HD camera. This down-facing camera records high definition video of the payload throughout the flight. The video provides visual evidence to verify the successful opening and closing of the sampling chambers, as well as diagnostic information when malfunctions occurred.

2.2. The LAMB payload

The LAMB payload that was flown for all experimental campaigns is shown in Fig. 1. The following sections provide details about the construction and operation of this payload.

2.2.1. Mechanical system

The main structural support of the payload is centered on the electronics box (Fig. 1), an aluminum framed structure which houses the control electronics, flight power supply, data storage, linear actuators for opening and closing sample chamber doors, and a GPS receiver and radio beacon for real time transmission of position and altitude coordinates. The dimensions of the box are approximately 25 cm ×25 cm and 20 cm high.

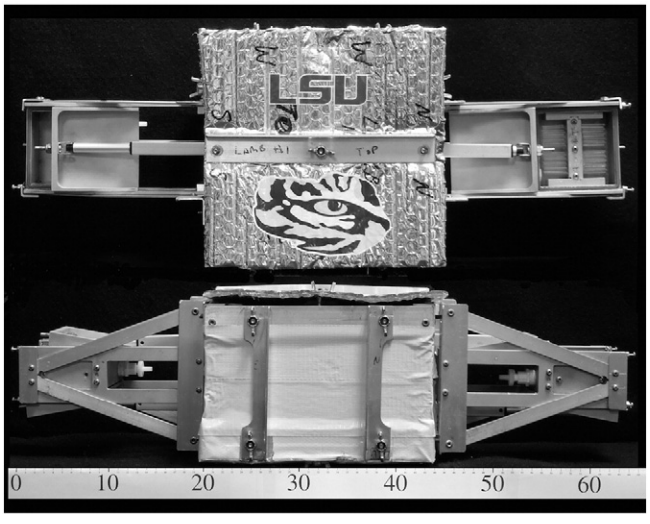

Fig. 1. A top and side view of the LAMB payload. The central electronics box includes the flight control, monitoring and power systems. Each payload includes two sampling chambers (one on the right and one on the left) and each chamber has two doors (top and bottom) that are operated by linear actuators. The top view shows the top door on the right hand side fully retracted exposing the sampling rods and rod holders. The third procedural control chamber is not pictured here. The scale bar is in cm.

Each sampling chamber was constructed of milled aluminum and the inner cross-sectional area of the chamber is 45 cm^2 (Fig. 1). The chambers are mounted between a pair of side rails, which are then connected to the electronics box. The upper and lower doors slide along a pair of grooves milled into the rails. The fixed ends of the actuators are connected to a center post in the electronics box and the moveable shafts of the actuators are connected to the chamber doors. Retracting the actuator shafts opens the chamber while extending them closes and seals the chamber. A Teflon™ coating was applied to reduce the sliding friction between the doors and the side rails.

Each detachable sampling chamber holds forty Rotorods® (IMS Health, Inc.), hereafter referred to as rods, that are secured in place by a rod holder shown in the top view image in Fig. 1. Each rod holder (6.0 cm × 1.3 cm) secures twenty rods spaced 0.25 cm apart, and two rod holders are staggered in each chamber. The rod holder position is maintained by shallow grooves milled on either side of the inner-chamber walls and is fixed in place by screws. Each rod (22 mm × 1.6 mm) has an impact-sampling surface of 35 mm^2. O-rings placed in grooves milled on the top and bottom surfaces of the chamber walls provide a seal when the doors are closed. A threaded Luer lock fitting was attached to the side of each chamber to accommodate a 0.22 μm syringe filter, allowing pressure equalization between ambient and the chamber interior when the chamber is sealed. A third, structurally identical control chamber, was flown in addition to the sampling payload (Fig. 1) for each mission.

The LAMB payload was modified for use on the High Altitude Student Platform (HASP, http://laspace.lsu.edu/hasp), a zero-pressure, high altitude balloon, and sampled for 8.4 h at 38 km in 2013. Procedural controls from eight flights during 2013, including HASP, were analyzed according to the methods described below.

2.2.2. Electronics and power supply

The LAMB payload electronics consist of a control and power system. The control system is responsible for monitoring payload altitude, actuator shaft position, actuator temperature, external temperature, internal temperature, external relative humidity, as well as controlling the opening and closing of the chamber doors at pre-programmed altitudes. The control system is comprised of an Arduino MEGA 2560 microcontroller, a custom GPS receiver–micro secure digital (SD) storage board, and an actuator control board. The boards are stacked and communicate across a bus interface. Connected to the control system's GPS unit is the secondary beaconing system, which is embedded in the payload and provides real time transmission of position and altitude coordinates. Like the primary, it is also a Byonics Micro-Trak and is specifically used as a backup to the primary beaconing system should it fail. This secondary beaconing system is also used to enhance position resolution as the payload nears the ground upon descent.

The Arduino MEGA 2560 microcontroller executes all instructions, digitizes up to 16 analog signals, controls all actuator input/output (I/O) functionality, and communicates with the external serial devices. It is also responsible for executing instructions based upon input from the GPS receiver, temperature and relative humidity sensors, as well as actuator shaft position data. All flight sensor and diagnostic data managed by the Arduino is written to files on the microSD card for post-flight analysis.

The actuator control board controls the four linear actuators (one for each chamber door). Power to each actuator is provided through an h-bridge integrated circuit chip, allowing the actuator to be extended and retracted by reversing the polarity between power and ground. A pair of I/O lines to the h-bridge allows control of the polarity for each actuator.

System power is provided by 10 lightweight Energizer Ultimate Lithium “AA” batteries wired in series to supply 15 to 18 VDC to power all

payload components, including the electronics and actuators. During flight, the average current draw from the batteries is 130 mA, but can range from 120 mA to 1300 mA depending upon whether the radio transmitter and door actuators are active. The battery pack is specified to supply 3.0 Ah at 0 °C (Energizer®, designation: ANSI 15-LF, IEC-FR6), which taking into account the duty cycles of the various powered components, allows the payload to operate autonomously for about 20 h.

2.2.3. Flight software

The payload is controlled by an embedded system and is designed to operate autonomously, making operational decisions based upon the data collected by the control system. At the heart of the control system is the Arduino MEGA microcontroller. A logic flow chart describing the software that runs on the microcontroller is shown in Fig. 2. The primary functions of the flight software are to collect positional information from the GPS receiver, command the linear actuators to open or close the sampling chamber doors at programmed altitudes, and to ensure that the doors are closed during payload or balloon failure modes. Further, the software records data from the multiple temperature sensors and a relative humidity sensor, with archiving by the software occurring every 3 s. Errors are logged together with critical information as they occur, so that in-flight problems can be analyzed after the flight. The flight control system software continuously polls the GPS receiver for a position string that contains, among other information, the longitude, latitude and altitude of the payload. A new position string should be available to the control system once every 3 s. Once the string is received, it is parsed, scanned for errors, and made sure to contain accurate positional data before it is logged and deemed usable. Only then is the position data used to determine the direction of motion of the payload, which requires several consecutive position strings that report motion in the same direction.

The sample chamber doors are opened only when the direction of motion is determined to be ascending, the minimum sampling altitude has been exceeded, the maximum sampling altitude has not been exceeded, and at least one valid position packet has been received within the last minute. If the doors are already open, they will be closed if the direction of motion is determined to be descent or if a valid position string has not been received for over 1 min (Fig. 2).

The system timestamps and logs 'event' records, status updates, and errors to the control system's on-board microSD card. The events are logged periodically while the errors and updates are logged as they occur. Timestamps are obtained from the GPS disciplined free-running system clock which is zeroed upon reboot. The time stamped archived data provides a complete and accurate timeline of the flight and provides information such as when doors are opened and closed, error diagnostics, and environmental parameters.

The event record contains the following information: the last position packet data, each door position recorded in millimeters, all actuator motor temperatures, interior payload temperatures, exterior payload temperature, and exterior relative humidity. The errors that are logged during normal execution of the code include: "microSD card initialization failure", "GPS position string buffer empty for over some time period", "GPS position string buffer out-of-bounds error", "position string parse error", "position string incorrect checksum error", "checksum calculation error", "descent warning — closing all doors", "unable to open/close door to its proper position", and "too much time has passed since the receipt of the last good positional packet — closing all doors". Some examples of status updates are: "door 1 was opened", "a new file was created on the microSD card", "a position string was received from the GPS receiver", etc.

2.2.4. Component and payload testing

To ensure that the pressure equalization of the sample chamber was through the syringe filter, each sampling chamber was sealed and a leak test was performed on all chambers. The chamber leak rate varied for each, but was always less than 0.05 kPa per min. The flow rate through the filter was determined to be approximately 5.0 kPa per min, two orders of magnitude greater than the leak rates measured for the sealed chambers.

Preflight system tests were also performed in a thermal vacuum chamber to simulate the low pressure and temperature conditions that the payload encounters during flight. During testing in the thermal vacuum chamber, the chambers were commanded opened and closed repeatedly and shown to operate correctly down to pressures of 1.1 kPa. In addition, a series of low temperature tests were conducted in a freezer to evaluate the effectiveness of the payload insulation to keep the payload electronics operational.

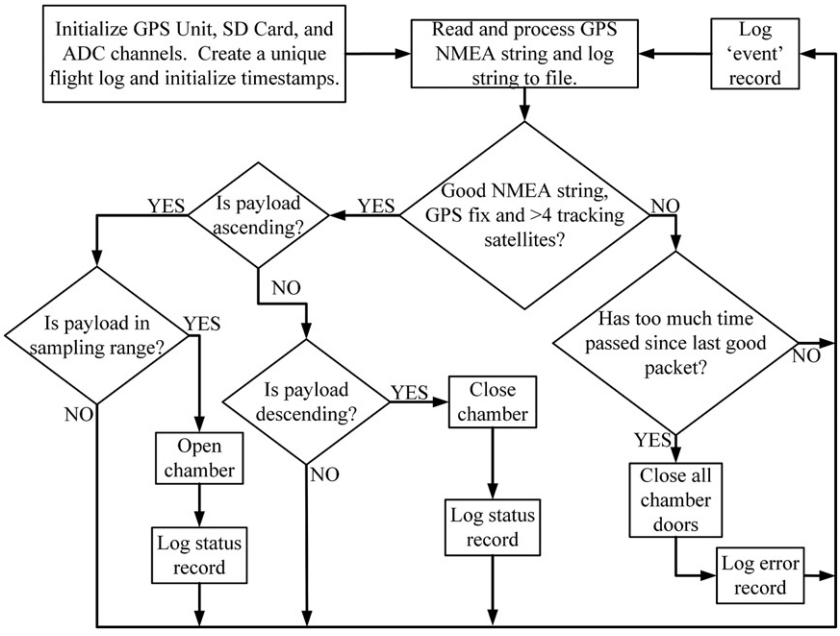

Fig. 2. Flow chart describing the logic flow of the autonomous embedded flight control system software. The system relies on accurate GPS data in order to open and close sampling chamber doors at predetermined altitudes. Errors are handled through the normal logic flow of the software. For example, if too much time passes since the last good GPS packet was received, the sampling chamber doors are closed. Once GPS packets are received again, the logic dictates that the doors will be opened if the payload is ascending and is in sampling range.

2.3. Microbiological analysis

2.3.1. Bacterial strains and culturing conditions

Cultures of *Bacillus atrophaeus* (ATCC 9372) were grown aerobically with shaking (250 rpm) overnight in 5.0 mL of tryptic soy broth (TSB, Difco™, cat. no.: DF0370-17-3) at 20 °C. An aliquot of *B. atrophaeus* was plated onto Schaeffer's sporulation media (Schaeffer et al., 1965) and incubated for five days at 20 °C. The presence of endospores was verified by phase contrast microscopy. The cell and endospore populations were harvested by centrifugation for 10 min. at 17,000 ×*g* and suspended in 1.0 mL of phosphate-buffered saline (PBS), followed by a second wash with 1.0 mL of PBS. *Deinococcus radiodurans* (ATCC 13939) was cultured aerobically overnight in 5.0 mL of TSB with shaking at 20 °C; the cells were harvested and suspended as described above. Suspensions of each bacterial culture were applied to the surface of triplicate rods and allowed to air dry for 1 h within the laminar flow hood.

For the flight control rods, the presence of viable microorganisms was assessed by placing the silicone-coated portion of each rod into a culture tube containing the liquid media R2A (Difco™, cat. no.: 218262), 1% R2A, TSB, and 1% TSB amended with 100 μg mL^{-1} cycloheximide (Acros Organics, cat. no: AC35720010) to inhibit the growth of fungi (Ha et al., 1995). Each rod was placed in media within 12 h of recovery and incubated at 4 °C ($n = 160$) for 60 days. Enrichment cultures were then shifted to 20 °C and monitored for 21 days. Over the course of 81 days, aliquots of the enrichments cultures were plated onto solid media (R2A and TSA) and monitored for colony growth at 20 °C.

2.3.2. Silicone coating of the sampling rods

All sides of the sampling rods were exposed to 1.3×10^5 μW cm^{-2} of germicidal ultraviolet radiation (UV-C; 254-nm) for 20 min., soaked in 2000 ppm sodium hypochlorite for 20 min., rinsed with 70% (v/v) ethanol, and allowed to dry in a laminar flow hood (Labconco, cat. no.: 3612504) for 1 h. The rods were subsequently coated in silicone grease (IMS Health, Inc.) by the method of Frenz et al. (2001). After 24–48 h, the rods were exposed to ethylene oxide (450–650 mg L^{-1}) for 4 h at 55 °C and a relative humidity of 30–50% (Ecosterile, Inc.).

2.3.3. Decontamination of rods inoculated with bacteria

Three rods containing cells of each bacterial strain were placed into 1 mL of PBS and serially diluted to determine the number of cells that remained viable after air-drying. This value was designated as the initial colony forming unit (CFU) concentration that each decontamination treatment was compared to. Ten-fold serial dilutions of each culture were spread plated onto tryptic soy agar (TSA, Difco™, cat. no.: 236590) and incubated at 20 °C. The total number of CFU was recorded after 72 h of growth. The average initial concentration of CFU for the individual treatments of ethylene oxide, UV-C, and sodium hypochlorite were 9.7×10^5 ($\pm 8.7 \times 10^4$, standard deviation, $n = 3$) and 1.7×10^6 ($\pm 6.0 \times 10^4$, $n = 3$) CFU rod^{-1} for *B. atrophaeus* and *D. radiodurans*, respectively. For the combined treatment, the average initial concentrations were 3.0×10^5 ($\pm 4.4 \times 10^5$, $n = 3$) and 4.9×10^7 ($\pm 6.8 \times 10^6$, $n = 3$) CFU rod^{-1} for *B. atrophaeus* and *D. radiodurans*, respectively. Additionally, inoculated rods were exposed to one of four treatments: ethylene oxide, UV-C, sodium hypochlorite, or a combined treatment of UV-C, sodium hypochlorite, and ethylene oxide. The samples were then placed into sterile Petri dishes and stored at 20 °C for 24 h.

After each treatment, cells on the rods were dislodged from the silicone grease by placing the rods into 1.0 mL of sterile PBS and vortexing the mixture for 10 min. The three replicates were ten-fold serially diluted and plated onto TSA, incubated at 20 °C, and the number of CFU was determined after 72 h. Assuming 100% removal of cells from the rods during vortexing and considering the number of CFU required for a standard dilution plate (i.e., between 30–300 CFU on a 100 mm diameter plate), the limit of quantification for our method was 300 CFU rod^{-1}. For samples that had <300 CFU, a value of 29 was substituted (Eaton et al., 1998), allowing calculation of the reduction in culturable cells for all treatments. The log reduction of CFU (or mol ATP; see below) after decontamination was calculated by subtracting the mean log density of the treated samples from the mean log density of the untreated, air-dried rods.

2.3.4. External cleaning of the chambers after recovery

Once the payload was recovered, all chambers were inspected to ensure that the doors had maintained a seal. The chambers were subsequently removed from the payload base and placed in clean plastic bags for return to a clean area for processing. All chambers were manipulated and opened in a portable laminar flow hood (Fungi Perfecti, LLC, Item no.: E-ALFH1). Prior to opening the chambers, all exposed surfaces were wiped down with 70% (v/v) ethanol to remove surface dust and debris encountered during flight and landing. The rod holders were aseptically removed from the chambers and placed into sterile Petri dishes for immediate processing (ATP analysis and culturing) or stored at −20 °C for subsequent analysis.

2.3.5. Direct counting of cells via epifluorescence microscopy

The number of DNA-containing cells on each flight control rod was estimated by staining with equal volumes of 0.22 μm-filtered Tris–borate–EDTA (1×) buffered SYBR™ Gold (Molecular Probes, Inc., cat. no. S-11494) and an antifade solution (0.1% phenylenediamine in a 1:1 solution of PBS and glycerol). A rod stage adaptor (IMS Health Inc.) was used to hold the samples and a 10 μL aliquot of the stain: antifade solution was applied directly to the surface of the rods, followed by the application of a coverslip. The samples were stained for 20 min. in the dark.

The cells were visualized with an Olympus bx51 epifluorescence microscope. For each rod, sixty random fields of view (FOV) were counted, with each FOV representing 2.8×10^4 μm^2. Fluorescing particles smaller than 0.7 μm were not counted because they were difficult to distinguish from autofluorescing particulates. The cell concentration per rod was calculated from the average number of cells per field and extrapolated to the total sampling area. The cell densities on 21 flight control rods, obtained from the seven August 2013 sampling missions, were determined using this method.

2.3.6. Measurement of the cellular adenosine triphosphate (ATP) concentration

To measure the concentration of ATP in cells attached to the inoculated and flight control rods, samples were analyzed using an ATP Biomass Kit HS (Biothema, Inc. cat. no. 266–112). An ATP solution (100 nmol L^{-1}) supplied by the manufacturer was diluted into 0.22 μm filtered, autoclaved deionized water (DIW) to generate a standard curve. Free ATP was removed by placing the rod into a 1:1 solution of 0.22 μm filtered, autoclaved DIW and ATP eliminating reagent (Biothema, Inc.), followed by incubation for 17 min at 20 °C. Cellular ATP was then extracted according to the manufacturer's instructions, the luciferase enzyme solution was added to the sample, and luminescence was measured using a 20/20n luminometer (Turner Biosystems, cat. no.: E5331). The light produced was measured in relative light units (RLUs) and converted to ATP concentration using the standard curve. Based on the addition of 1.0×10^3 pmol of the ATP standard to each sample, there was no sign of inhibition of the reaction from the samples when compared to the addition of the standard to water. A total of 96 flight control rods from seven flights during August 2013 were quantified for cellular ATP within 12 h of sampling.

2.3.7. Total particle concentration and characterization

Six rods from the August 2013 flight controls were prepared for scanning electron microscopy by sputter coating with gold/palladium for 4 min to apply a layer that was approximately 1.0 Å thick. Particles embedded in the silicone grease were enumerated using a JSM-6610LV scanning electron microscope under the high vacuum mode

(−0.8 kPa). Sixty randomly chosen FOV (each FOV represents 1.3×10^4 μm^2) for each rod were examined at a voltage of 10–12 kV. A digital image of each FOV was captured and the particle boundaries were traced and analyzed using ImageJ software (Schneider et al., 2012). The area, perimeter, major and minor axis lengths, and circularity for each particle were measured. Circularity was calculated by the following formula (Royston-Bishop et al., 2005; Schneider et al., 2012):

$$\text{Circularity} = \frac{4\pi * \text{area}}{\text{perimeter}^2}. \quad (1)$$

2.4. Statistical analyses

Statistical analyses were performed using StatPlus:mac statistical analysis software (AnalystSoft, Inc.) and SAS® University Edition (SAS Institute Inc., copyright, 2014). Student's t-test was used to compare the mean log density of samples to the mean log density of the controls, and when the variances were not equal, the heteroscedastic Student's t-test was used. The one-way ANOVA, with post hoc Tukey–Kramer test, was utilized to compare the effectiveness of the decontamination treatments. All data were normalized to account for differences in the initial CFU concentrations and are reported as the mean (± the standard deviation) of the log-transformed data.

To determine the limits of detections for each assay, the data were first checked for the possibility of a nonparametric distribution. The data are reported as the mean (± the standard error of the mean) calculated by the SAS software using the PROC GLIMMIX statement with the negative binomial distribution and Kenward–Roger adjustments.

3. Results

3.1. Reduction of cellular viability and ATP by the decontamination methods

To examine the effectiveness of several decontamination methods on the reduction of microbial cells and their associated molecules from the sampling rods, a series of experiments were conducted. Fig. 3 shows the log reduction in CFU and mol of ATP after rod decontamination by UV-C, ethylene oxide, sodium hypochlorite, and a combination of all three treatments. In these experiments, 10^5 to 10^7 CFU mL^{-1} of the type strains *B. atrophaeus* and *D. radiodurans* were applied to rod surfaces and the survival of the cells and persistence of cellular ATP was quantified.

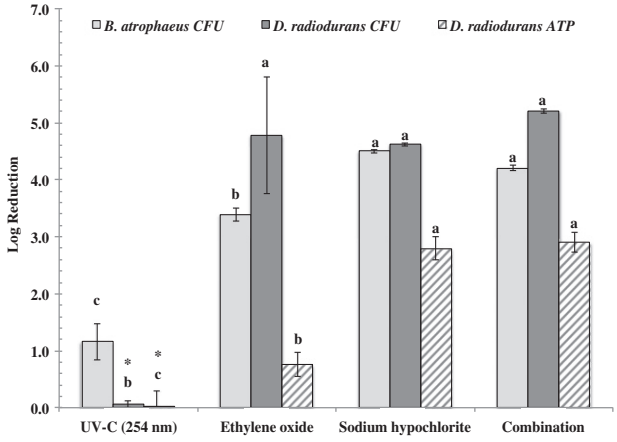

Fig. 3. Reduction of bacterial culturability and ATP on rods decontaminated by ethylene oxide, UV-C, sodium hypochlorite, and a combination of all three. Each value represents the mean and the error bars indicate the standard deviation (CFU, $n = 3$; ATP, $n = 5$). The letters a–c rank the treatments for each sample and are based on one-way ANOVA with post hoc Tukey–Kramer analysis. Asterisks represent p values that were not statistically different from the controls ($p > 0.05$; heteroscedastic Student's t-test).

In Fig. 3, sodium hypochlorite and the combination treatments were the most effective decontamination methods for reducing culturable cells of *B. atrophaeus* (3.4 ± 0.11 log units) and *D. radiodurans* (4.8 ± 1.0 log units), as well as cellular ATP from *D. radiodurans* (0.76 ± 0.21 log units). Statistical analysis revealed that ethylene oxide was as successful as sodium hypochlorite and the combined treatments in the reduction of *D. radiodurans* CFU (Fig. 3, indicated by the treatments labeled with a lower case "a"). Ethylene oxide was significantly less effective than sodium hypochlorite and the combined treatments in the reduction of *B. atrophaeus* CFU and *D. radiodurans* ATP (Fig. 3, indicated by the lower case "b"). UV-C was the least effective decontamination treatment for either analyte. Although the concentration of CFU rod^{-1} for *B. atrophaeus* was significantly reduced by the UV-C treatment (1.2 ± 0.32 log units, $p = 0.02$), rods inoculated with *D. radiodurans* were not statistically different from the CFU rod^{-1} or the concentration of ATP from control samples (Fig. 3, indicated by the asterisks). A single ATP data point from the decontamination experiment (specifically, the sodium hypochlorite treatment; $n = 4$) was deemed to be an extreme outlier (greater than three deviations from the mean) and was subsequently removed from the analysis.

3.2. Balloon missions

One flight test was conducted in May 2013 at the NASA Columbia Scientific Balloon Facility (CSBF) balloon launch site near Palestine, TX and seven additional flights were completed in August 2013 at the NASA CSBF launch site near Fort Sumner, New Mexico. During these flights, the payload was shown to operate correctly up to an altitude of 38 km. Following recovery of the balloon payloads, the recorded diagnostic data and flight video were examined to assess payload performance. The flight video verified that the chamber top doors always opened at the pre-programmed altitude. The chamber bottom doors, however, usually required several attempts before a successful opening was achieved.

Key diagnostic parameters for one test flight are shown in Fig. 4, plotted against Mission Elapsed Time (MET) in units of hours and minutes. In panel A, the altitude profile for the test flight (solid black line) shows a fairly consistent ascent up to about 30 km, where the flight was terminated at ~1:22 MET and the payload began its descent on parachute. The external temperature data (dark gray line) shows a profile typical of these altitudes with the coldest temperatures (−48 to −51 °C) occurring when the vehicle passes through the tropopause at 0:39 MET on ascent and again at 1:30 MET on descent. The constant temperature indicated by the flat line occurring at 1:30 MET indicates that the payload experienced colder temperatures that were out of sensor range (<−51 °C) during the descent. The internal temperature (light gray line) remained above 0 °C, consistent with the temperature time constant seen during laboratory testing. The temperature of the linear actuators dipped as low as −35 °C and continued to operate correctly, opening and sealing the chambers in extreme cold conditions. Panel B of Fig. 4 shows the chamber door positions recorded during the flight and the sequence of chamber door operation, which was verified with the flight video. The top doors on both chambers opened as expected upon command, but when sampling in the stratosphere, there was a delay in opening the bottom doors. This effect is presumably due to chilling of the chambers as the payload passed through the tropopause, increasing the door seal resistance. Nevertheless, a few minutes of solar heating of the bottom door after the top door opened were sufficient to resolve the problem. The plot in panel C of Fig. 4 indicates the occurrence of an unexpected error during the flight from diagnostic information recorded on-board the payload. For this flight, a single GPS error was recorded, indicating that a valid GPS string was not properly received or processed for at least 60 but not more than 63 seconds. Had the sample chamber doors been open at the time that this error occurred, they would have closed and reopened once a normal and valid GPS string receipt resumed. However, the error occurred after the set

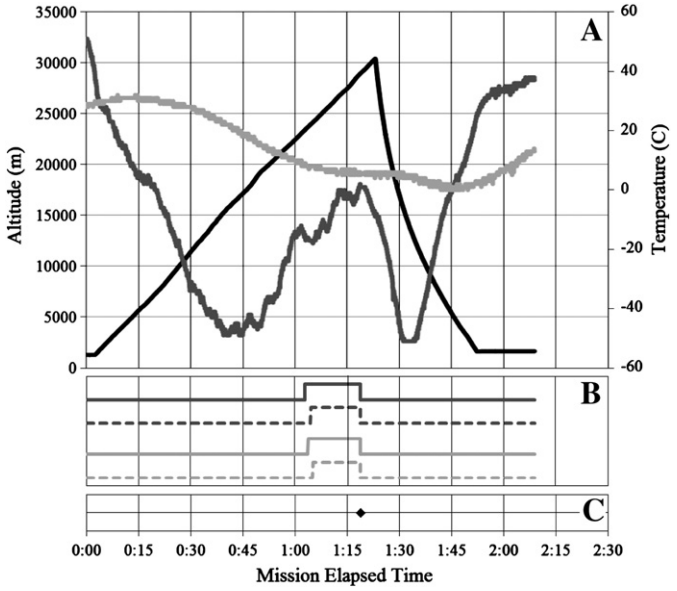

Fig. 4. Key flight diagnostic parameters from the test flight, ACES-42. The x-axis is Mission Elapsed Time (MET) in units of hours and minutes starting with launch at 0:00. Panel A shows the payload's altitude (black line), the internal temperature (light gray line) and the external temperature (dark gray line). Panel B shows the opening and closing of the chamber doors. Chamber one's doors are represented by the dark gray lines while chamber two's are represented by the light gray lines. The solid lines represent the top chamber doors while the dashed lines represent the bottom doors. Panel C of the figure shows the occurrence(s) of unexpected errors of which there was only one during this flight.

maximum sampling altitude was exceeded, and therefore, no action was taken.

3.3. Determination of detection limits for cell and molecular analysis

As a result of the May 2013 flight, it was determined the flight control rods did not receive microbial contamination during flight or landing that was significantly higher than the sampling rods that never left the confines of the laboratory. Using microscopic examination, it was determined that there was not a significant difference between the cell ($p = 0.77$, $n = 6$) and ATP ($p = 0.06$, $n = 17$) concentrations between the flight and laboratory controls.

The cell, ATP, and particle concentration data distributions were positively skewed and all had variances greater than their respective means, indicating negative binomial distributions. The number of cells per rod ranged from 260 to 750 and averaged 520 (± 29, $n = 21$) cells per rod. A total of 530 bacterial cells were counted from 21 independent rods, subsampled from 7 different flight controls. With a mode of zero, 95% of the FOV counted contained two or fewer cells. Only two FOV contained four cells, the highest number of cells counted per FOV. Based on limits of detection at 3-sigma and the epifluorescence microscopy data, our decontamination protocol allows the detection of as few as 87 cells per rod (Table 1). The average concentration of cellular ATP on the flight control rods was 7.5×10^{-16} ($\pm 0.85 \times 10^{-17}$ mol rod^{-1}, $n = 96$) and an ATP concentration greater than 2.6×10^{-16} mol rod^{-1} provides a 3σ confidence level of detection above the background. Since an entire rod can be placed into a single culture tube with liquid media, one colony-forming unit per rod is theoretically sufficient to detect growth. Of the 160-flight control rods placed into enrichment culture, growth was observed in only 1 of these cultures during the course of this study.

A total of 58 particles were counted from six flight control rods that flew on two separate flights. Particles on these rods ranged from 1.0 to 13 μm in diameter, with a mode of 3.9 μm. Of the particles measured, 95% were smaller than 11 μm in diameter. The number of particles counted in 60 FOV for each rod ranged from 1.0 to 29 and the average concentration of particles rod^{-1} was 480 ($\pm 2.0 \times 10^2$). The average particle area and major axis length (diameter) were 12 (± 1.7) μm^2 and 4.4 (± 0.33) μm, respectively. In Eq. (1), a perfect circle has a value of 1.0. The average circularity of the particles analyzed on flight control rods was 0.74 (± 0.11). In order to achieve a signal 3-sigma above the controls, a total of 6.0×10^2 particles must be collected per rod (Table 1).

Table 1
Limits of detection for microbiological and particulate analyses conducted on decontaminated rod surfaces.

Measurement	Method	3σ limit of detection above the flight control rods
Total cell concentration	SYBR Gold™ enumeration	87 cells ($n = 21$)
Viable cells and biomass	ATP quantification	2.6×10^{-16} mol ATP or 85 cells[a] ($n = 96$)
Culturable cells	Liquid enrichment	1 colony forming unit[b] ($n = 160$)
Total particle concentration	SEM enumeration	600 particles ($n = 6$)

[a] Based on an estimated 3.0×10^{-18} mol of ATP per bacterial cell (Franzen and Binkley, 1961).
[b] Theoretical limit based on the ability of 1 viable CFU on each rod to enumerate in culture media.

4. Discussion

Microbial aerosol sampling at altitudes above the atmospheric boundary layer (~1 km above sea level) can be conducted from mountaintop observatories (Amato et al., 2005; Bowers et al., 2009; Smith et al., 2012, 2013; Xia et al., 2013), using aircraft (DeLeon-Rodriguez et al., 2013; Griffin, 2004; Smith et al., 2010), or high altitude balloon platforms (Harris et al., 2002; Rogers and Meier, 1936; Yang et al., 2008). Although a ground-based approach provides obvious advantages, including the ability to sample large volumes of air, the air masses may be influenced by surface level interactions (Xia et al., 2013) and sampling is restricted to altitudes in the troposphere. Aircraft based sampling for microorganisms has been accomplished up to altitudes of 20 km (DeLeon-Rodriguez et al., 2013; Griffin, 2004; Smith et al., 2010), providing the necessary flexibility to examine vertical profiles in the atmosphere and allowing large air volumes to be sampled. For example, DeLeon-Rodriguez et al. (2013) filtered 2.2 to 15 m^3 of air at altitudes of 3.0 to 10 km for their microbiological analysis. While aircraft-based platforms have distinct advantages for characterizing the spatial and temporal variability of microbial aerosols in the Earth–atmosphere system, they are also limited by the fact that sampling has been restricted to altitudes below ~20 km and an aircraft requires enormous financial and logistic support resources.

Balloon-based approaches to detect and describe microbes in the stratosphere were first attempted over 75 years ago (Rogers and Meier, 1936). To date, most of the high altitude studies have focused on detecting only culturable microorganisms, which is an approach well known to bias for a minor fraction of the total microbial diversity (Staley and Konopka, 1985; Stewart, 2012). In cloud water samples enriched at 5 °C and 17 °C, less than 0.28% of the total bacterial cells were found to be cultured using standard methods (Vaïtilingom et al., 2012). It is also important to note that strategies used previously in the sampling of stratospheric microbes have not provided data on the quantitative abundance of microorganisms or assessed the level of background contamination associated with flight operations and subsequent analysis. For example, Harris et al. (2002) used liquid neon-cooled cryopumps to sample at altitudes from 19–41 km and reported the presence of one to three microscopic cell "clumps" per sample. However, since the amount of air sampled during these missions is

not known, relating the abundance of the bioaerosols to the source air mass is not possible. Further, Yang et al. (2008) report the recovery of two CFU from filters that concentrated 0.35 m^3 of air at 20–30 km, but in the absence of procedural controls and repeat measurements, it is difficult to prove that such results represent bona fide recoveries of stratospheric microbes rather than artifacts resulting from contamination.

Given the state of knowledge in the field of high altitude microbiology and the inherent challenges involved, our objective was to develop a quantitative sampling strategy that collected microbial aerosols from defined air mass volumes and sampled multiple altitude ranges per mission. Equally important for this effort was to establish protocols that assessed the cleanliness of the payload and sampling substrates, allowing the authenticity of results obtained from atmospheric sampling to be verified. To sample bioaerosols in the high atmosphere, we adapted the Rotorod impaction sampling method (Frenz et al., 1996) and developed a light weight device that could sample while ascending through the atmosphere or through rotation at a fixed altitude. The sampling chambers hold up to 40 individual rods, providing the opportunity for replication of measurements and purposing the samples to various types of microbiological and molecular analyses. Since the payload samples at altitudes where the atmospheric pressure is 50 to 100 times lower than that at sea level, a complete seal on the chambers would create an undesirable situation where a partial vacuum would be created in the chamber interior when the payload returned to surface pressure. In this scenario, an uncontrolled leak could allow extraneous microbes to enter the chamber and contaminate the sample. To prevent this, we equipped each chamber with a syringe filter to establish a "controlled leak" that equalizes the chamber interior and exterior pressure while preventing all particles >0.22 μm from entering the sampling chamber.

The volume of air sampled by a single rod is the area of its upward facing side (35 mm^2) multiplied by the change in altitude during its sampling flight path, with each rod passing through 0.035 m^3 per km of altitude sampled. The efficiency at which aerosols are collected on a rod is a function of the ascent rate (5.8 m s^{-1}) and particle size. For example, the collection efficiency for 6.0 μm particles traveling at 5.0 m s^{-1} was 56% (Frenz, 1999), but decreased to 0.5% for particles 0.5 to 1.0 μm in diameter (Magill et al., 1968). Hence, owing to the small volumes sampled, efficiency of the rod collection method, and the minimum thresholds required to overcome the signal to noise ratio (Table 1), the altitudinal resolution of our approach is low. Based on previous reports of cell concentrations between 1.5 and 10 km (10^4 to 10^5 cells m^{-3}; Amato et al., 2005; DeLeon-Rodriguez et al., 2013; Xia et al., 2013), the minimum vertical resolution necessary to breach the detection limit for cells 6.0 μm in diameter (Table 1) by our method is 0.5 km in a tropospheric air mass.

The ability of the sampling chambers to keep samples pristine during balloon missions was evaluated by flying sampling chambers that remained sealed, providing procedural control data for each mission. Background contamination on the procedural controls was determined to not be significantly different from identical rods that were not removed from the laboratory, indicating that the chambers were effective at excluding external microbial contamination during all phases of launch and recovery. The abundance of cellular and molecular contamination associated with our procedural controls allowed us to estimate the level of detection for various parameters important to microbial aerosol characterization (Table 1). Detection of viable microbial biomass in the atmosphere via the quantification of cellular ATP will require at least 2.6×10^{-16} mol of ATP, which corresponds to ~85 viable bacterial cells per rod (based on 3.0×10^{-18} mol of ATP per bacterial cell; Franzen and Binkley, 1961). This was nearly identical to the cell concentration values (87 DNA-containing cells per rod) required to exceed the background threshold for epifluorescent microscopy. Based on data for particles in the size range of 0.5 to 10.4 μm, a collection of 600 particles would be sufficient to achieve a signal above the controls. It is important to note that measurable quantities of cells and their molecules (i.e., ATP) remained detectable after decontamination procedures. Therefore, the parallel analysis of procedural controls is an important consideration when measuring microbial concentrations that approach the signal to noise ratio.

The levels of detection reported in Table 1 could presumably be lowered if the background level of cells and molecules were reduced by more effective decontamination methods. High temperature combustion or autoclaving were not possible with all the materials we used, specifically the rods. Therefore, we evaluated the effectiveness of sodium hypochlorite, UV-C irradiation, and ethylene oxide for microbial disinfection of the materials. In these tests, we chose *B. atrophaeus* because its endospores have shown high levels of resistance to ethylene oxide treatment (Mosely et al., 2005) and *D. radiodurans*, which is extremely resistant to UV-C and desiccation (Bauermeister et al., 2011). Therefore, the decontamination data presented here should be considered a conservative estimate of microbial survival under these conditions.

A variety of biological molecules commonly used as proxies for microbial biomass (e.g., ATP; Vaïtilingom et al., 2012) and diversity (DNA; DeLeon-Rodriguez et al., 2013) can persist, even in materials that have been sterilized (Venkateswaran et al., 2003). Therefore, the ability to eliminate and assess the level of biochemical contamination was important. There was not a significant difference between the sodium hypochlorite and the combined treatments. The use of sodium hypochlorite alone would be a viable option if payload materials were not compatible with UV-C or ethylene oxide sterilization. Although ethylene oxide was less effective at decreasing the viability of endospores and concentration of cellular ATP than sodium hypochlorite, it is an effective decontamination method to consider in applications that are incompatible with sodium hypochlorite. Sodium hypochlorite offers several advantages for use as a chemical decontaminant; it is inexpensive, readily available, and easily adaptable for field-based protocols.

Environmental conditions recorded during balloon flights indicated that the payload functioned at pressures and temperatures as low as 0.7 kPa and −51 °C, respectively. The primary reason the payload configuration that we present here possesses only two sampling chambers is to remain compliant with weight restrictions specified by the United States Federal Aviation Administration (Code of Federal Regulations, title 14, sec. 101.1). It is possible to fly larger weight payloads, at the expense of a much more complicated flight system and flight authorization process, making it possible to increase the sampling capacity and accommodate additional sample chambers per payload. In addition, the payload can be adapted for float sampling. We sampled with LAMB for ~8 h while at float altitude (38 km) by rotating the payload on a fixed axis, allowing the sampling of ~2.0 m^3 per rod. As such, the payload that we describe here can be adapted to sample microbial aerosols on any type of balloon platform.

In conclusion, we have developed a robust and reliable approach for the quantitative sampling of microbial aerosols at altitudes in the troposphere and stratosphere. Data from procedural controls flown on actual balloon missions allowed us to demarcate the limits of detection for microbial cells and their associated molecules. In addition to providing data on the upper limits of Earth's biosphere and geographical movement of microorganisms on a global scale, the integration of microbiology into high altitude balloon research also has relevance to astrobiology. The properties of microbes surviving extreme combinations of pressure, temperature, relative humidity, and UV irradiation are important for assessing the habitability of other planetary environments. Further, our research is also relevant to discussions regarding the prevention of forward contamination during future extraterrestrial missions, where sample integrity will be a fundamental concern (e.g., Christner et al., 2005; Eigenbrode et al., 2009; Venkateswaran et al., 2004).

Acknowledgments

This work was supported by a grant from the National Aeronautics and Space Administration Experimental Program to Stimulate Competitive Research (NNX10AN07A) and the Louisiana Board of Regents (NASA/LEQSF(2010-13)-Phase3-04). Partial support was also provided by a LaSPACE Fellowship Award (N.B.) under the Louisiana Space Consortium program (NASA NNX104I40H) and through a National Science Foundation grant 1241161 (B. C.). D. Branch, S. Burke, J. Giammanco, S.B. Ellison, C. Jones and S. Junot assisted with the payload design, construction, and testing.

References

Amato, P., Ménager, M., Sancelme, M., Laj, P., Mailhot, G., Delort, A.-M., 2005. Microbial population in cloud water at the Puy de Dôme: implications for chemistry of clouds. Atmos. Environ. 39, 4143–4153.

AnalystSoft, d. StatPlus:mac — statistical analysis program for Mac OS. Version 2009See http://www.analystsoft.com/en/.

Bauer, H., Kasper-Giebl, A., Löflund, M., Giebl, H., Hitzenberger, R., Zibuschka, F., Puxbaum, H., 2002. The contribution of bacteria and fungal spores to organic carbon content of cloud water, precipitation and aerosols. Atmos. Res. 64, 109–119.

Bauermeister, A., Moeller, R., Reitz, G., Sommer, S., Rettberg, P., 2011. Effect of relative humidity on *Deinococcus radiodurans*' resistance to prolonged desiccation, heat, ionizing, germicidal, and environmentally relevant UV radiation. Microb. Ecol. 61, 715–722.

Bowers, R.M., Lauber, C.L., Wiedinmyer, C., Hamady, M., Haller, A.G., Fall, R., Knight, R., Fierer, N., 2009. Characterization of airborne microbial communities at a high-elevation site and their potential to act as atmospheric ice nuclei. Appl. Environ. Microbiol. 75, 5121–5130.

Burrows, S., Butler, T., Jöckel, P., Tost, H., Kerkweg, A., Pöschl, U., 2009. Bacteria in the global atmosphere — part 2: modeling of emissions and transport between different ecosystems. Atmos. Chem. Phys. 9, 9281–9297.

Christner, B., Mikucki, J., Foreman, C., Denson, J., Priscu, J., 2005. Glacial ice cores: a model system for developing extraterrestrial decontamination protocols. Icarus 174, 572–584.

Christner, B., Morris, C., Foreman, C., Cai, R., Sands, D., 2008. Ubiquity of biological ice nucleators in snowfall. Science 319, 1214.

DeLeon-Rodriguez, N., Lathem, T., Rodriguez-R, L., Barazesh, J., Anderson, B., Beyersdorf, A. , Ziemba, L., Bergin, M., Nenes, A., Konstantinidis, K., 2013. Microbiome of the upper troposphere: species composition and prevalence, effects of tropical storms and atmospheric implications. Proc. Natl. Acad. Sci. U. S. A. 110, 2575–2580.

Eigenbrode, J., Benning, L.G., Maule, J., Wainwright, N., Steele, A., Amundsen, H.E.F., the AMASE 2006 Team, 2009. A field-based cleaning protocol for sampling devices used in life-detection studies. Astrobiology 9, 455–465.

Eaton, A.D., Clesceri, L.S., Greenberg, A.E., Franson, M.A.H., 1998. American Public Health Association American Water Works Association Water Environment Federation, 1998. Standard methods for the examination of water and wastewater. American Public Health Association, Washington, DC.

Franzen, J.S., Binkley, S.B., 1961. Comparison of the acid soluble nucleotides in *Escherichia coli* at different growth rates. J. Biol. Chem. 236, 515–519.

Frenz, D., 1999. Comparing pollen and spore counts collected with the Rotorod® Sampler and Burkard spore trap. Ann. Allergy Asthma Immunol. 83, 341–349.

Frenz, D., Scamehorn, R.T., Hokanson, J.M., Murray, L.W., 1996. A brief method for analyzing Rotorod® samples for pollen content. Aerobiologia 12, 51–54.

Frenz, D., Guthrie, B., Straka, J., 2001. A rapid, reproducible method for coating Rotorod® Sampler collector rods with silicone grease. Ann. Allergy Asthma Immunol. 87, 390–393.

Fulton, J.D., 1966. Microorganisms of the upper atmosphere. III. Relationship between altitude and micropopulation. Appl. Microbiol. 14, 238–240.

Griffin, D., 2004. Terrestrial microorganisms at an altitude of 20,000 m in Earth's atmosphere. Aerobiologia 20, 135–140.

Griffin, D.W., 2008. Non-spore forming eubacteria at an altitude of 20,000 meters in Earth's atmosphere: extended incubation periods needed for culture based assays. Aerobiologia 24, 19–25.

Griffin, D., Garrison, V., Herman, J., Shinn, E., 2001. African desert dust in the Caribbean atmosphere: microbiology and public health. Aerobiology 17, 203–213.

Griffin, D.W., Westphal, D.L., Gray, M.A., 2006. Airborne microorganisms in the African desert dust corridor over the mid-Atlantic ridge, Ocean Drilling Program, Leg 209. Aerobiologia 22, 211–226.

Ha, S.S., Pillai, K. Maciorwski, Ricke, S.C., 1995. Cycloheximide as a media amendment for enumerating bacterial populations in animal feeds. J. Rapid Meth. Autom. Microbiol. 4, 95–105.

Hara, K., Zhang, D., 2012. Bacterial abundance and viability in long-range transported dust. Atmos. Environ. 47, 20–25.

Harris, M., Wickramasinghe, N., Lloyd, D., Narlikar, J., Rajaratnam, P., Turner, M., Al-Mufti, S., Wallis, M., Ramadurai, S., Hoyle, F., 2002. The detection of living cells in the stratosphere. Proc. SPIE 4495, 192–198.

Huffman, J., Treutlein, B., Pöschl, U., 2010. Fluorescent biological aerosol particle concentrations and size distributions measured with an ultraviolet aerodynamic particle sizer (UV-APS) in Central Europe. Atmos. Chem. Phys. 10, 3215–3233.

Huffman, J., Sinha, B., Garland, R., Snee-Pollmann, A., Gunthe, S., Artaxo, P., Martin, S., Andreae, M., Pöschl, U., 2012. Size distributions and temporal variation of biological aerosol particles in the rainforest characterized by microscopy and real-time UV-APS fluorescence techniques during AMAZE-08. Atmos. Chem. Phys. 12, 11997–12019.

Imshenetsky, A.A., Lysenko, S.V., Kazakov, G.A., 1978. Upper boundary of the biosphere. Appl. Environ. Microbiol. 35, 1–5.

Joly, M., Amato, P., Deguillaume, L., Monier, M., Hoose, C., Delort, A.-M., 2014. Direct quantification of total and biological ice nuclei in cloud water. Atmos. Chem. Phys. 14, 8185–8195.

Magill, P.L., Lumpkins, E.D., Arveson, J.S., 1968. A system for appraising airborne populations of pollens and spores. Am. Ind. Hyg. Assoc. J. 29, 293–298.

Mosely, G., Gills, J., Krushefski, G., 2005. Evaluating the formulae for the integrated lethality in ethylene oxide sterilization using six different endospore forming strains of bacteria, and comparisons of integrated lethality of ethylene oxide and steam systems. PDA J. Pharm. Sci. Technol. 59, 64–86.

Murata, K., Zhang, D., 2014. Transport of bacterial cells toward the Pacific in Northern Hemisphere westerly winds. Atmos. Environ. 87, 138–145.

Pöschl, U., Martin, S., Sinha, B., Chen, Q., Gunthe, S., Huffman, J., Borrmann, S., Farmer, D., Garland, R., Helas, G., Jimenez, J., King, S., Manzi, A., Mikhailov, E., Pauliquevis, T., Petters, M., Prenni, A., Roldin, P., Rose, D., Schneider, J., Su, H., Zorn, S., Artaxo, P., Andreae, M., 2010. Rainforest aerosols as biogenic nuclei of clouds and precipitation in the Amazon. Science 329, 1513–1515.

Rogers, L.A., Meier, F.C., 1936. U.S. Army Air Corps Stratosphere Flight of 1935 in the Balloon "Explorer II". The National Geographic Society, Washington, D.C.

Royston-Bishop, G., Priscu, J., Tranter, M., Christner, B., Siegert, M., Lee, V., 2005. Incorporation of particulates into glacial accreted ice above Subglacial Lake Vostok, Antarctica. Ann. Glaciol. 40, 145–150.

SAS® University Edition, SAS Institute Inc., Cary, NC, copyright 2014. See http://www.sas.com/en_us/software/university-edition.html.

Sattler, B., Puxbaum, H., Psenner, R., 2001. Bacterial growth in supercooled cloud droplets. Geophys. Res. Lett. 28, 239–242.

Schaeffer, P., Millet, J., Aubert, J.-P., 1965. Catabolic repression of bacterial sporulation. Proc. Natl. Acad. Sci. U. S. A. 54, 704–711.

Schneider, C., Rasband, W., Eliceiri, K., 2012. NIH Image to ImageJ: 25 years of image analysis. Nat. Methods 9, 671–675.

Shivaji, S., Chaturvedi, P., Suresh, K., Reddy, G., Dutt, C., Wainwright, M., Narlikar, J., Bhargava, P., 2006. *Bacillus aerius* sp. nov., *Bacillus aerophilus* sp. nov., *Bacillus stratosphericus* sp. nov., and *Bacillus altitudinis* sp. nov., isolated from cryogenic tubes for collecting air samples from high altitudes. Int. J. Syst. Evol. Microbiol. 56, 1465–1473.

Smith, D.J., Griffin, D.W., Schuerger, A.C., 2010. Stratospheric microbiology at 20 km over the Pacific Ocean. Aerobiologia 26, 35–46.

Smith, D., Jaffe, D., Birmele, M., Griffin, D., Schuerger, A., Hee, J., Roberts, M., 2012. Free tropospheric transport of microorganisms from Asia to North America. Appl. Microb. Ecol. 64, 973–985.

Smith, D., Timonen, H., Jaffe, D., Griffin, D., Birmele, M., Perry, K., Ward, P., Roberts, M., 2013. Intercontinental dispersal of bacteria and archea by transpacific winds. Appl. Environ. Microbiol. 79, 1134–1139.

Staley, J.T., Konopka, A., 1985. Measurements of in situ activities of nonphotosynthetic microorganisms in aquatic and terrestrial habitats. Annu. Rev. Microbiol. 39, 321–346.

Stewart, E.J., 2012. Growing unculturable bacteria. J. Bacteriol. 194, 4151–4160.

United States National Archives and Records Administration. Code of Federal Regulations. Title 14. Aeronautics and Space. Section 101, subpart A. 79, 2009

Vaïtilingom, M., Charbouillot, T., Deguillaume, L., Maisonobe, R., Parazols, M., Amato, P., Sancelme, M., Delort, A.-M., 2011. Atmospheric chemistry of carboxylic acids: microbial implication versus photochemistry. Atmos. Chem. Phys. 11, 8721–8733.

Vaïtilingom, M., Attard, E., Gaiani, N., Sancelme, M., Deguillaume, L., Flossman, A., Amato, P., Delort, A.-M., 2012. Long-term features of cloud microbiology at the Puy de Dôme (France). Atmos. Environ. 56, 88–100.

Venkateswaran, K., Hattori, N., La Duc, M.T., Kern, R., 2003. ATP as a biomarker of viable microorganisms in clean-room facilities. J. Microbiol. Meth. 52, 367–377.

Venkateswaran, K., Chung, S., Allton, J., Kern, R., 2004. Evaluation of various cleaning methods to remove *Bacillus* spores from spacecraft hardware materials. Astrobiology 4, 377–390.

Wainwright, M., Wickramasinghe, N., Narlikar, J., Rajaratnam, P., 2003. Microorganisms cultured from stratospheric air samples obtained at 41 km. FEMS Microbiol. Lett. 218, 161–165.

Xia, Y., Conen, F., Alewell, C., 2013. Total bacterial number concentration in free tropospheric air above the Alps. Aerobiologia 29, 153–159.

Yang, Y., Yokobori, S., Kawaguchi, J., Yamagami, T., Iijima, I., Izutsu, N., Fuke, H., Saitoh, Y., Matsuzaka, Y., Namiki, M., Ohta, S., Toriumi, M., Yamada, K., Seo, M., Yamagishi, A., 2008. Investigation of cultivable microorganisms in the stratosphere collected by using a balloon in 2005. JAXA research and Development Report, JAXA-RR-08-001, pp. 35–42.